Cobalt–molybdenum sulfide catalysts prepared by *in situ* activation of bimetallic (Co–Mo) alkylthiomolybdates

H. Nava[a], C. Ornelas[a], A. Aguilar[a], G. Berhault[b], S. Fuentes[c], and G. Alonso[a,*]

[a] *Departamento de Catálisis, Centro de Investigación en Materiales Avanzados, Chihuahua, C.P. 31109, Chihuahua, México*
[b] *Laboratoire de Catalyse en Chimie Organique, UMR 6503 CNRS, Université de Poitiers, 40 Avenue du Recteur Pineau, 86022 Poitiers cedex, France*
[c] *Departamento de Catálisis, Centro de Ciencias de la Materia Condensada (CCMC), UNAM, Apartado Postal 2681, 22830 Ensenada, B.C., México*

Received 9 August 2002; accepted 16 December 2002

Unsupported cobalt–molybdenum sulfide catalysts were prepared from bimetallic CoMo alkyl precursors by *in situ* activation during the hydrodesulfurization (HDS) of dibenzothiophene (DBT). The bimetallic CoMo precursors were prepared by reaction of tetraalkylammonium thiomolybdate salts, $(R_4N)_2MoS_4$ (where R = H, methyl, butyl, pentyl or hexyl), with $CoCl_2$ in water at a Co/Mo molar ratio of 0.3. These catalysts exhibit a "Swiss-cheese"-like morphology, high surface areas (from 52 up to 320 m^2/g), high content of carbon (C/Mo = 2.2–3.3) and type IV adsorption–desorption isotherms of nitrogen. The *in situ* activation of these tetraalkylammonium thiobimetalate precursors leads to a mesoporous structure with pore size ranging from 2 to 4.5 nm. X-ray diffraction showed that the structure of unsupported cobalt–molybdenum sulfide catalysts corresponds to a poorly crystalline structure characteristic of 2H-MoS_2 with low-stacked layers. The nature of the alkyl group strongly affects both the surface area and the HDS activity. The catalytic activity is strongly enhanced when using carbon-containing precursors; the CoMo catalysts prepared by *in situ* activation of $Co/[N(C_4H_9)_4]_2MoS_4$ presents the highest HDS activity. The highest surface area of the catalysts was observed for the CoMo catalyst formed from $Co/[N(C_6H_{13})_4N]_2MoS_4$.

KEY WORDS: bimetallic precursors; *in situ* activation; hydrodesulfurization; CoMo catalysts.

1. Introduction

Catalysis by transition metal sulfides (TMS) plays a crucial role in the petroleum industry. Owing to their exceptional resistance to poisons, TMS are unique catalysts for the removal of heteroelements (S, N, O) in the presence of a large amount of hydrogen. Hydrodesulfurization (HDS) of organic molecules such as thiophene, benzothiophene and dibenzothiophene (DBT) is generally performed with molybdenum or tungsten sulfides supported on alumina and promoted by Group VIIIB elements (cobalt or nickel) with a promoter atomic ratio Co(Ni)/[Co(Ni) + Mo(W)] between 0.2 and 0.4 [1,2].

The synergetic effect of Co or Ni on the catalytic activity of the Mo and W sulfides has been well documented [3–5]. The promoter effect of cobalt in Mo sulfide catalysts for HDS reactions has been attributed to the amount of Co atoms that can be accommodated on the edges of MoS_2 layers and also to the electronic transfer that Co induces on Mo atoms located at these sites [6,7]. Model calculations have shown that the Sabatier principle of molecules bonding at the surface (not too strong, not too weak) is well adapted to explain the volcano periodic dependence of the catalytic activity of metal sulfides versus the position of the metal in the periodic table [8]. In this respect, cobalt promotion weakens the metal–sulfur bond strength up to the optimum range for HDS activity.

The way in which Co is introduced on the MoS_2 catalyst has an influence on the catalytic properties. Cobalt- or nickel-promoted unsupported HDS catalysts have been prepared by different methods, including comaceration [9] and homogeneous sulfide precipitation [6]. The catalytic properties of Co/MoS_2 obtained by these methods are reported to depend strongly on the processing atmosphere and also on the heating conditions [10,11].

The thiosalt decomposition method has been widely used in the preparation of molybdenum and tungsten sulfide catalysts for hydrotreating reactions [12,13]. Indeed, thiosalt decomposition is a very effective and reproducible alternative method for obtaining better catalysts; the thiosalts have sulfur already bound to the metal atoms in a tetrahedral coordination, and their decomposition has been reported to undergo a topotactic reaction, whereby the *c*-axis of sulfide remains the same as in the precursor [14]. In this respect, the *in situ* decomposition of ammonium tetrathiomolybdate, $(NH_4)_2MoS_4$, is an effective method to produce active phases, mainly for hydrogenation reactions as suggested by Yoneyama and Song [15]. Moreover, cobalt-promoted unsupported catalysts prepared from the decomposition of thiosalts have shown higher catalytic activities than catalysts prepared by other techniques [16,17].

---

[*] To whom correspondence should be addressed.
E-mail: gabriel.alonso@cimav.edu.mx

The method of *in situ* decomposition of monometallic and bimetallic tetraalkylammonium thiosalts [18–20] involving a sulfur-containing organic compound in hydrocarbon solution, pressurized with hydrogen and heated to 623 K, yields active metal sulfides. This mode of decomposition leads to materials containing certain amounts of carbon and described with the general formula $MoS_{2-y}C_z$, where $0.01 < y < 0.5$ and $0.01 < z < 3.0$ [21]. These catalysts exhibit improved activity for the HDS of DBT [22]. The role of carbon in the formulation of those HDS catalysts is not completely obvious, but it is possible that carbon, at least partly, is included in the arrangement of active sites [23–25]. Moreover, it was shown recently that molybdenum carbide has high activity in hydroprocessing reactions [26,27]. Mo_2C/Al_2O_3 produced by carburizing alumina-supported ammonium molybdate in a CH_4/H_2 reactant stream showed three times higher activity in HDS process than MoS_2/Al_2O_3 catalyst [27].

In this work, Co-promoted MoS_2 catalysts were prepared from bimetallic Co–Mo alkyl precursors by *in situ* activation during the HDS of DBT. Five types of molybdenum thiosalt precursors, $(NR_4)_2MoS_4$ (where R = H, methyl, butyl, pentyl, and hexyl), were reacted with $CoCl_2$ to obtain the bimetallic precursors. The *in situ* activation technique was used to obtain bimetallic CoMo catalysts, referred as CoMo-R (where R = H, C_1, C_4, C_5, C_6). Catalysts were characterized by XRD, BET nitrogen adsorption and SEM after catalytic evaluation.

2. Experimental

2.1. Bimetallic precursor preparation

The preparation of bimetallic precursors was carried out in two steps. In the first step, the preparation of tetraalkylammonium thiomolybdate precursors, $(NR_4)_2MoS_4$ (R = H, methyl, butyl, pentyl and hexyl), was carried out according to the method reported previously by Alonso and co-workers [28–31]. In the second step, the molybdenum precursor was mixed with $CoCl_2$ in aqueous solution at a 30% molar Co/Mo ratio to obtain five bimetallic precursors.

The appropriate amount of thiomolybdate precursors, $(NR_4)_2MoS_4$ to yield 1 g of MoS_2 {1.6 g of ammonium thiomolybdate, $(NH_4)_2MoS_4$, in 20 ml of water, 2.3 g of tetramethylammonium thiomolybdate, $[(CH_3)_4N]_2MoS_4$), in 20 ml of water, 4.4 g of tetrabutylammonium thiomolybdate, $[(C_4H_9)_4N]_2MoS_4$, in 50 ml of water, 5.1 g of tetrapentylammonium thiomolybdate, $[(C_5H_{11})_4N]_2MoS_4$, in 60 ml of a 1 : 5 methanol–water solution, 5.8 g of tetrahexylammonium thiomolybdate, $[(C_6H_{13})_4N]_2MoS_4$, in 100 ml of a 1 : 5 methanol–water solution} was added under stirring at room temperature to a second solution of 0.47 g of $CoCl_2 \cdot \frac{1}{2}H_2O$ dissolved in 10 ml of water; immediately precipitates were formed. The five bimetallic salts were filtered and dried at room temperature.

The final bimetallic precursor was amorphous in nature and unstable in air or water. Consequently, crystallographic determination of the structure was not possible. However, the Co/Mo molar ratio of 0.3 was in agreement with a hypothetical stoichiometry $(R_4N)_4Co(MoS_4)_3$. In this case, a stoichiometric reaction would be:

$$3(R_4N)_2MoS_4 + CoCl_2 \longrightarrow (R_4N)_4Co(MoS_4)_3 + 2(R_4N)Cl.$$

However, owing to the amorphous character of these precursors, in the present study these bimetallic thiosalts will only be labeled $Co/[(NR_4)_2MoS_4]$. This instability could be related to a previous study by Pan *et al.* [32] on the formation of $(R_4N)_3Co(MoS_4)_2$ thiosalts which are unstable in air. In our case, the $(R_4N)_4Co(MoS_4)_3$ thiosalt is probably transformed into an amorphous polymeric structure of the type $Co_x(MoS_4)_{3x}$ keeping a Co/Mo ratio of 0.3.

2.2. Catalytic activity and selectivity

The HDS of DBT was carried out in a Parr Model 4522 high-pressure batch reactor. The appropriate amount of bimetallic precursor to yield 1.0 g of CoMo-R catalyst was placed in the reactor with the HDS reactant (5.0 vol% of DBT in decalin). Each bimetallic precursor was prepared in tablet form by uniaxial pressing and was crushed in a mortar before placing it inside the reactor. The reactor was then pressurized to 3.1 MPa with hydrogen and heated to 623 K at a rate of 10 K/min. After the working temperature had been reached, sampling for chromatographic analysis was performed during the course of each run to determine the conversion *versus* time dependence. The reaction run time averaged about 5 h. The reaction products were analyzed using a Perkin-Elmer Auto-system chromatograph with a 1.83 mm × 32 mm i.d. packed column containing OV-3 (phenyl methyl dimethyl silicone, 10% phenyl) as a separating phase.

The main reaction products from the HDS of DBT are biphenyl (BP) and phenylcyclohexane (PCH). The selectivity for the main reaction products (BP, PCH) was determined for CoMo-R catalysts prepared for each bimetallic precursor and was calculated for a given product as the weight percentage of the product in the product mixture. The mean standard deviation for catalytic measurements was about 5%.

2.3. Catalyst characterization

Characterization of catalysts was performed on samples obtained after the catalytic tests. The samples were separated from the reaction mixture by filtration, then washed with 2-propanol to remove residual hydrocarbons and dried at room temperature.

A Jeol JSM5800 IV scanning electron microscope was used to perform morphology and EDX elemental analyses. Several fields were analyzed at different magnifications in order to aid in recognition of the prevalent features. EDX analysis was performed using an eBX-ZAF system. MoS_2 reference compounds were used to deconvolute L lines of S and L lines of Mo.

Specific surface area determinations were performed with a Quantachrome AUTOSORB-1 by nitrogen adsorption at 77 K using the BET isotherm. Samples were degassed under flowing argon at 473 K for 2 h before nitrogen adsorption. The pore distribution was obtained from the desorption isotherm following the BJH method. The mean standard deviation for surface area measurements was about 2%.

X-ray diffraction (XRD) studies were carried out in a Phillips X Pert MPD diffractometer, equipped with a curved graphite monochromator, using CuKα radiation ($\lambda = 1.54056$ Å) operating at 43 kV and 30 mA.

3. Results

3.1. Elemental analysis

The Co/Mo, S/Mo and C/Mo atomic ratios determined using EDX analysis are reported in table 1. A crystalline MoS_2 flake was used for calibration of Mo and S signals. The Co/Mo atomic ratio for all catalysts remained almost constant at a value of around 0.3 whereas the S/Mo ratio varied from 1.8 to 2.2. High amounts of carbon ($2.2 \leq C/Mo \leq 3.3$) were detected on all catalysts prepared by DBT HDS *in situ* decomposition of tetraalkylammonium salts. CoMo-H formed from ammonium tetrathiomolybdate (ATM), $(NH_4)_2MoS_4$ during the HDS of DBT already presents a high amount of C (C/Mo = 2.2). This result is noticeably higher than that observed previously for non-promoted MoS_2 catalyst *in situ* prepared under the same conditions (C/Mo = 0.5) [28]. The amount of carbon hardly changes with the type of alkyl precursor. The high amount of residual carbon may be present in the structure and also on the surface of the catalysts.

3.2. Surface area and pore size distribution

The size of the alkyl group in the bimetallic precursor has an important effect on the surface area and the total pore volume of the catalysts (*cf.* table 1).

The total pore volume exhibits a direct correlation with the length of the organic chain of the precursor since the total pore volume increases from 0.09 cm^3/g for CoMo-H to 0.32 cm^3/g for CoMo-C_6.

Table 1
Specific surface areas, total pore volume and elemental analysis of Mo, S, and C atomic ratios for *in situ* prepared CoMo sulfide catalysts

CoMo-R catalyst	Surface area (m^2/g)	Total pore volume (cm^3/g)	EDX analysis
CoMo-H	53	0.09	$MoS_{2.2}Co_{0.32}C_{2.2}$
CoMo-C_1	117	0.17	$MoS_{2.1}Co_{0.31}C_{3.1}$
CoMo-C_4	253	0.23	$MoS_{1.8}Co_{0.3}C_{3.1}$
CoMo-C_5	231	0.21	$MoS_{2.1}Co_{0.33}C_{3.3}$
CoMo-C_6	320	0.32	$MoS_{2.2}Co_{0.37}C_{3.3}$

As shown in figure 1, for CoMo-H catalyst, a poor developed porous system is observed with a low surface area of 53 m^2/g and a type I isotherm. The presence of alkyl groups in the precursor compound led to the development of porous systems with type IV isotherms. However, the CoMo-C_1 catalyst still presents an intermediate situation with a small hysteresis loop. Its surface area (117 m^2/g) is higher than that for the CoMo-H catalyst but still much smaller than that for the CoMo-C_4 catalyst. CoMo-C_4 presents a developed porous organization with an average pore diameter centered around 30 Å (*cf.* figure 2). Nevertheless, even though CoMo-C_4 shows a high surface area (253 m^2/g), its moderate pore volume (0.23 cm^3/g) indicates that microporosity still contributes to the total surface area. This sample exhibits a broad distribution of mesopores since the slope of the adsorption branch remains almost constant above $P/P_0 = 0.5$. Compared with CoMo-C_4, the CoMo-C_5 catalyst presents a relatively similar situation with comparable values for surface area and total pore volume. However, the hysteresis loop appears less developed and a narrower pore size distribution is obtained centered at a slightly larger pore diameter (35 Å). Finally, the CoMo-C_6 catalyst exhibits the highest surface area (320 m^2/g) and pore volume (0.32 cm^3/g). Its pore size distribution is much broader than that for CoMo-C_5 with contributions from wider mesopores.

The hysteresis loops shown by these catalysts correspond mainly to cylindrical pores open at both ends. However, some mesopores have narrow ends as in an ink-bottle pore shape, particularly for the CoMo-C_4 catalyst. CoMo-C_6 presents a less steep desorption branch, probably indicating a less narrow neck compared with the interior body of the pores.

3.3. Scanning electron microscopy

Images of the CoMo catalysts prepared from (a) $Co/(NH_4)_2MoS_4$, (b) $Co/[(N(CH_3)_4]_2MoS_4$, (c) $Co/[(N(C_4H_9)_4]_2MoS_4$, (d) $Co/[(N(C_5H_{11})_4]_2MoS_4$ and (e) $Co/[N(C_6H_{13})_4]_2MoS_4$ are reported figure 3. With the exception of CoMo-H, all these solids appear very porous with cavities probably resulting from the elimination of gas products occurring during the course

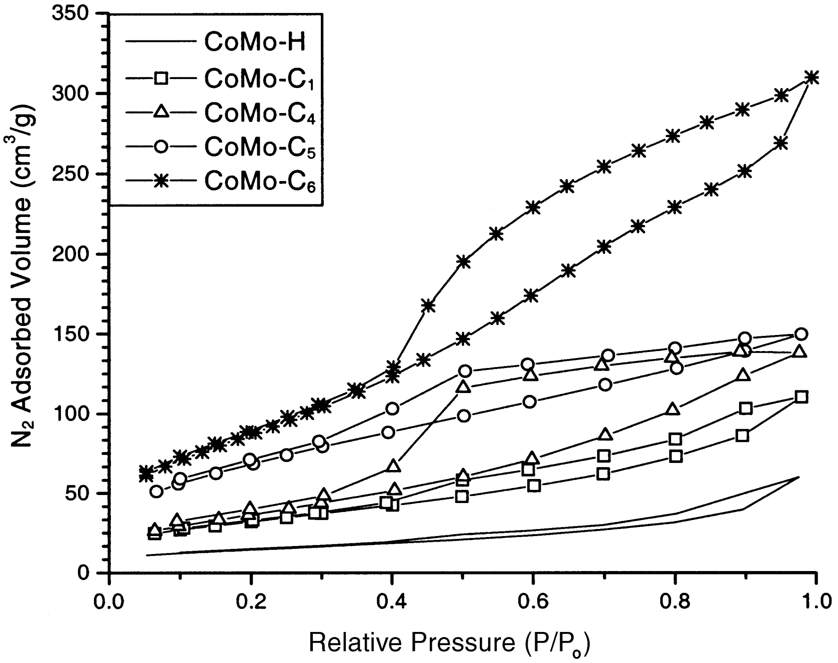

Figure 1. Adsorption–desorption isotherms for CoMo catalysts formed by *in situ* decomposition of the different thiobimetalate precursors.

of the decomposition process. For CoMo-C_1, only a few cavities are observed, which is in agreement with the presence of a poorly developed porous organization. CoMo-C_4 cavities seem to be formed by the agglomeration of small particles whereas for CoMo-C_5 the cavities are more uniform. Finally, the CoMo-C_6 images reveal a more disordered structure, in agreement with a broader pore size distribution.

3.4. *X-ray diffraction*

Figure 4 shows the XRD patterns of the CoMo-R catalysts prepared from the different tetraalkylammonium thiosalt precursors. All these patterns are in agreement with those reported for the poorly crystalline MoS_2 structure [33] with a weak (002) diffraction peak at $2\Theta = 14^\circ$ particularly for the CoMo-H and CoMo-C_1

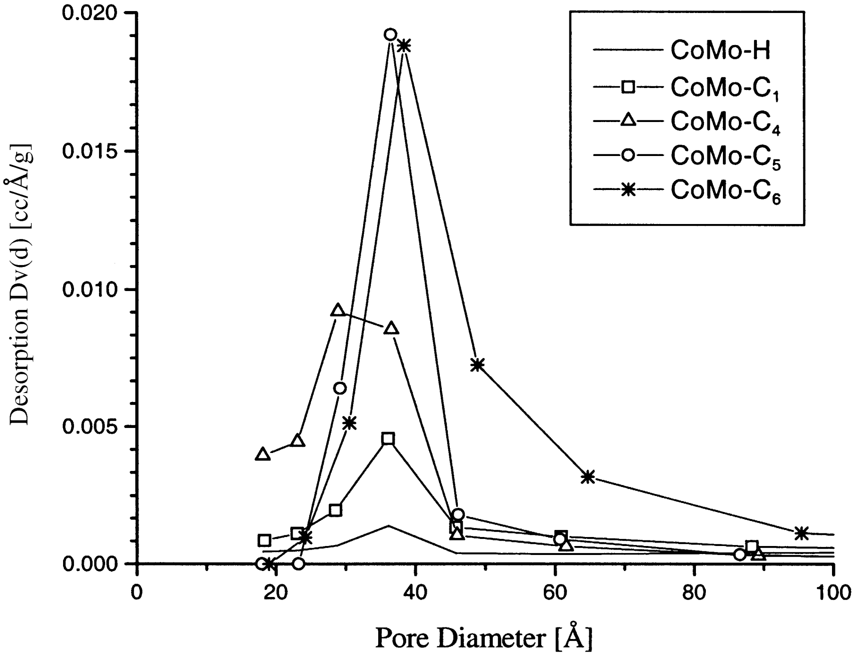

Figure 2. BJH pore size distribution of CoMo catalysts formed by *in situ* decomposition of the different thiobimetalate precursors.

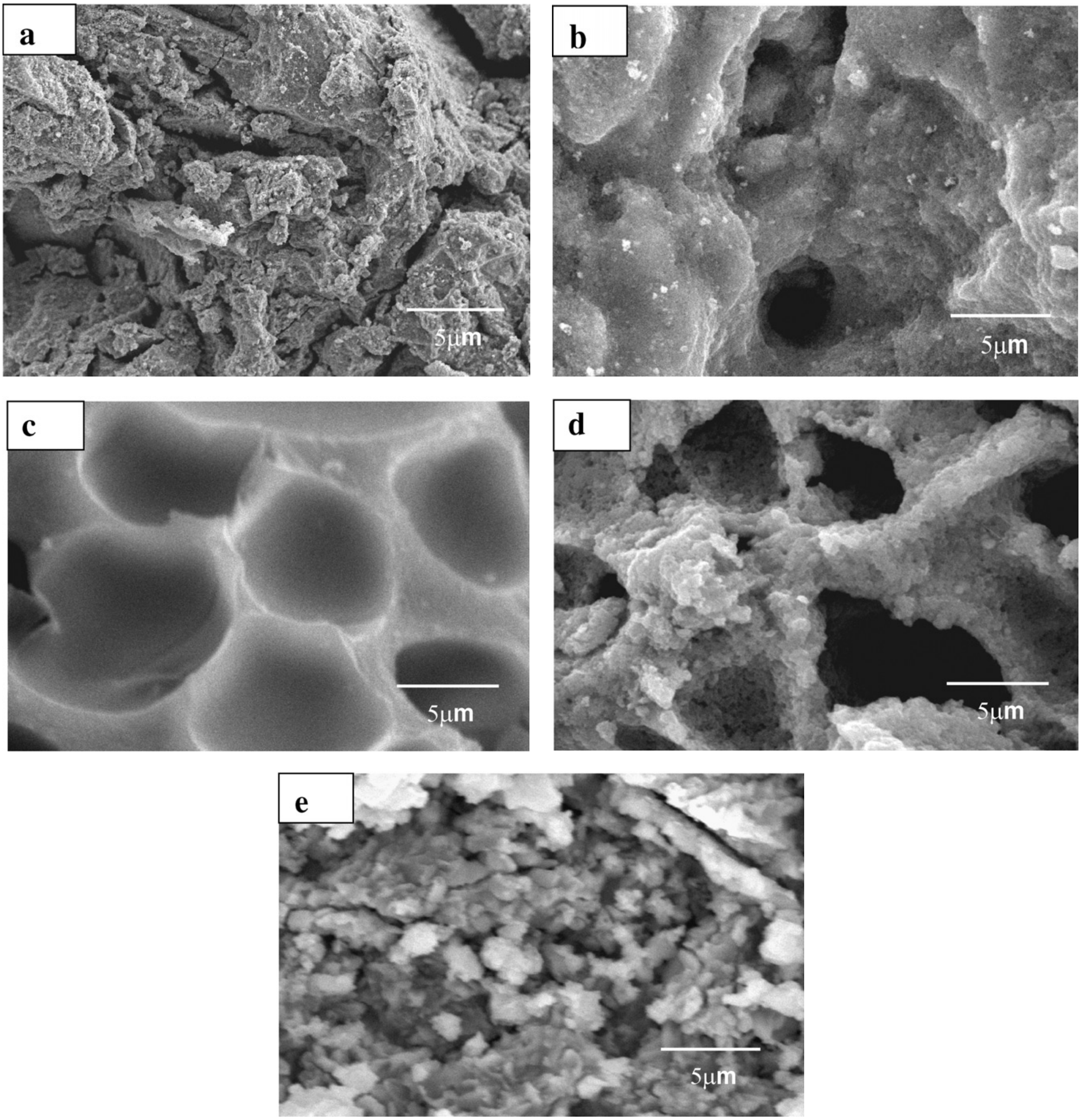

Figure 3. Scanning electron micrographs of the CoMo catalysts prepared from (a) Co/$(NH_4)_2MoS_4$, (b) Co/$[N(CH_3)_4]_2MoS_4$, (c) Co/$[N(C_4H_9)_4]_2MoS_4$, (d) Co/$[N(C_5H_{11})_4]_2MoS_4$, and (e) Co/$[N(C_6H_{13})_4]_2MoS_4$.

catalysts. However, a slight increase in intensity of the (002) peak is observed for CoMo-C_4, CoMo-C_5 and CoMo-C_6. Accordingly, the *c* direction layer stacking for all catalysts is representative of partly exfoliated samples. No peaks corresponding to cobalt sulfide phases were detected, indicating that Co is very well dispersed in the poorly crystalline structure of MoS_2.

3.5. Catalytic activity and selectivity

The HDS of DBT yields two main products: biphenyl (BP) through the so-called direct desulfurization pathway (DDS) and phenylcyclohexane (PCH) through the hydrogenative pathway (HYD). Phenylcyclohexane is a secondary product along this pathway obtained by C–S bond breaking reaction from tetrahydrodibenzothiophene (THDBT), an intermediate product formed by hydrogenation of one of the aromatic rings of dibenzothiophene. Since these two pathways are parallel [34], the ratio between HYD and DDS can be approximated in terms of the experimental selectivity by means of the equation

$$\mathrm{HYD/DDS} = (\mathrm{PCH})/(\mathrm{BP}).$$

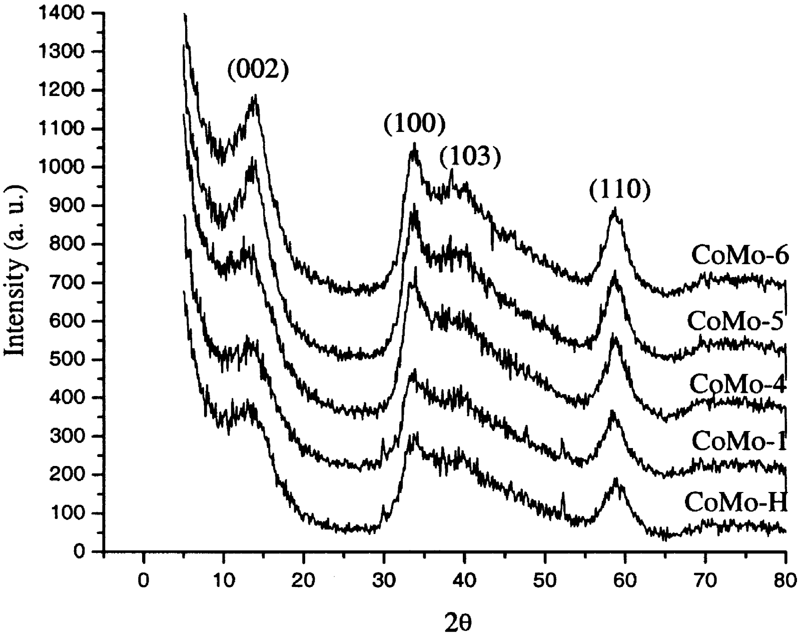

Figure 4. XRD patterns of CoMo catalysts formed by *in situ* decomposition of the different thiobimetalate precursors.

Table 2 summarizes the activity results and selectivity for BP and PCH through HYD/DDS ratios measured for different CoMo-R catalysts formed by the *in situ* decomposition of tetraalkylammonium thiobimetalate precursors. Initial rate constants were determined assuming, as for alkylammonium thiomolybdates, a complete decomposition of these precursors before the temperature of 623 K for the DBT HDS test [28]. The higher reactivity and tendency for decomposition of Co-containing alkylammonium thiomolybdates compared with "Mo only" alkylammonium thiosalts support this assumption.

Compared with the CoMo-H catalyst formed from Co/[$(NH_4)_2MoS_4$], the presence of an alkyl group in the precursor leads to a strong increase in activity even for the CoMo-C_1 catalyst. CoMo-C_4 with the highest HDS activity is 83% more active than CoMo-H. For longer alkyl groups, a slight decrease is observed but the activity is still much higher than for the CoMo catalyst prepared without the presence of alkyl groups in the bimetallic precursors.

Table 2
Initial rate constants, selectivity (HYD/DDS ratio) and [THDBT]/[BP] ratio of Co/MoS_2 catalysts prepared by *in situ* decomposition of tetraalkylammonium precursors during the HDS reaction of DBT ($T = 623$ K, $P = 3.1$ MPa)

CoMo-R catalyst	k (specific) ($\times 10^{-7}$ mol/g s)	HYD/DDS ratio	THDBT/BP ratio
CoMo-H	9.41	0.35	0.0599
CoMo-C_1	15.4	0.41	0.0291
CoMo-C_4	17.3	0.57	0.0374
CoMo-C_5	13.6	0.47	0.0456
CoMo-C_6	14.2	0.55	0.0092

The HYD/DDS ratio is slightly higher for CoMo catalysts prepared from precursors containing alkyl groups than for the CoMo-H catalyst. However, among the different CoMo-R catalysts, no real change in this ratio is detectable with increasing alkyl length in the initial precursor. Nevertheless, changes between hydrogenating and hydrogenolysis (C–S bond breakage ability) functions can be better ascertained when comparing THDBT and BP, which are the primary products along the two parallel pathways. Indeed, THDBT is formed only by the hydrogenation of one of the aromatic rings of DBT while BP is produced by direct C–S bond cleavage from DBT. In this case, the THDBT/BP ratio does not reveal any distinct change between hydrogenating and hydrogenolysis functions up to CoMo-C_5. A strong decrease in this ratio is observed for the CoMo-C_6 catalyst.

4. Discussion

The *in situ* activation of tetraalkylammonium thiometalates during the hydrodesulfurization of dibenzothiophene was used to generate non-promoted active MoS_2-based catalysts [28]. This mode of preparation leads to materials presenting high surface area, mesoporosity, large amounts of carbon and high catalytic activity. Here, such a method was extended to the preparation of CoMo sulfides through the use of tetraalkylammonium thiobimetalate precursors. In agreement with previous results for MoS_2 catalysts, very high surface area, mesopore size distributions and high C/Mo ratios (from 3.1 to 3.3) are also obtained.

The alkyl group present in the tetraalkylammonium precursor has a direct influence on surface area, total pore volume and HDS catalytic activity. Increasing the alkyl length from methyl to hexyl results in a marked increase in both the surface area from 117 to 320 m^2/g and the total pore volume from 0.17 to 0.32 cm^3/g. This increase in surface area is accompanied by the progressive formation of a mesoporous organization with an average pore diameter shifting somewhat to higher values when the length of the organic chain in the tetraalkylammonium precursor increases. More interestingly, tetraaalkylammonium bimetallic precursors lead systematically to a strong increase in HDS activity compared with non-carbon-containing ammonium bimetallic precursors even for the methyl group. Even if a dispersing effect of the active phase thanks to higher surface area could not be ruled out when explaining the increase in activity, no direct correlation can be observed between surface area and HDS activity. For instance, the CoMo-C_1 catalyst presents an HDS activity relatively similar to that of the CoMo-C_6 catalyst whereas their respective surface areas are very different (117 m^2/g for CoMo-C_1 *versus* 320 m^2/g for CoMo-C_6) (*cf*. tables 1 and 2). This situation is common for anisotropic layered materials such as MoS_2 and this represents a major ongoing challenge in this field. In the same way, the development of a mesoporous organization could not be invoked since the highest HDS activity is observed for the CoMo-C_4 catalyst, which still possesses a modest organized mesoporous structure in comparison with the CoMo-C_5 catalyst. In fact, this result supports the idea of a positive role of carbon in hydrotreating applications, as demonstrated by Chianelli and Berhault [35]. Indeed, in typical hydrotreating conditions, carbide and sulfide catalysts would tend to a common active surface presenting both S and C moieties, as already reported by different authors [22–24,36–38]. The formation of surface carbide-like entities was clearly observed by Berhault and co-workers [24,25] using NEXAFS on MoS_2 catalyzing the HDS of DBT. Consequently, the formation of "structural" carbon replacing surface sulfur atoms at the edges of the layers and taking part in the active phase may be envisaged in the present case. It should also be emphasized that a high amount of carbon is already detected on the CoMo-H catalyst (C/Mo = 2.2), but the amount stays smaller than that on the CoMo-R (R = alkyl) catalysts (C/Mo = 3.1–3.3). One might consider that when using tetraalkylammonium salts, the increase in HDS activity could be related to a more efficient interaction of carbon since it is already included in the precursor compound before the HDS test. Finally, one should emphasize that the amount of carbon detected could be present either at the surface of the catalyst (structural carbon) or as a support (excess carbon). Then, differentiation between a structural or a morphological role of carbon in this situation is not possible.

CoMo-R catalysts (Co/Mo molar ratio = 0.3) present higher catalytic activities (2–3 times) than their MoS_2 counterparts prepared from the equivalent monometallic tetraalkylammonium precursor. This demonstrates that Co included in the alkyl precursor induces a promoter effect on MoS_2. However, it should be pointed out that this synergetic effect is relatively weak in comparison with their alumina-supported equivalents. Excess carbon could be responsible for this low synergism, hampering the interaction between Mo and Co by blocking the migration of some Co species to the edges of the MoS_2 layers. However, a commercial CoMo/Al_2O_3 catalyst (Syncat CRITERION) has a similar activity value to the CoMo-C_4 catalyst ($k = 18.0$ *versus* 17.3×10^{-7} mol/g/s), showing that cobalt promoter actually contributes to higher active systems even if synergistic effects should be improved in future studies.

The HDS of DBT proceeds along two parallel pathways, the so-called direct desulfurization route (DDS) leading to biphenyl and the so-called hydrogenative route (HYD) leading to phenylcyclohexane via tetrahydrodibenzothiophene. The HYD/DDS ratio for MoS_2 catalysts prepared by *in situ* decomposition of ammonium tetrathiomolybdate during the HDS of DBT is much higher than the value observed in this study for the CoMo counterpart, *i.e.*, CoMo-H. This value decreases from 1.5 for MoS_2 (ex-ATM) to 0.35 for CoMo-H. Therefore, the cobalt promotion not only increases the activity but also modifies the selectivity along the two pathways. Cobalt strongly enhances the direct desulfurization route to biphenyl. This result is in agreement with previous results obtained on alumina-supported catalysts [39]. In fact, as reported by Breysse *et al.* [40], the opening of the C–S bond occurs through an elimination process. This mechanism involves the attack of a hydrogen atom (in the β-position relative to the sulfur atom in the organic molecule) by an anion acting as a basic site. Enhancement of the basicity of sulfur anions on freshly prepared CoMoS phase has been demonstrated by IR experiments [41] and could participate in this improvement of the DDS pathway.

The effect of the alkyl group initially present in the precursor on the selectivity does not appear obvious. Even if a slight increase of the HYD/DDS ratio is observed for carbon-containing precursors, the effect stays small. As revealed by the XRD results, the evolution of the (002) peak intensity indicates a slight increase in the stacking along the *c* direction, particularly when passing from a butyl to a pentyl group (see figure 4). According to the Rim-Edge model [42], in this case, a slightly more DDS favored selectivity would be expected since "rim" sites at the exterior of the stacked layers would be responsible for both C–S bond breaking and hydrogenation whereas "edge" sites located on "internal" stacked layers are only active for C–S bond breaking reactions. However, this is not observed here since the stacking increase stays weak. From a strict point of view, it should be emphasized that the Rim-Edge model was proposed for non-promoted unsupported MoS_2 catalysts and should not be applied to cobalt-promoted systems. The extension of this selectivity/stacking correlation to promoted catalysts has still to be done. However, applicable or not to the present case, a selectivity/stacking correlation as in the Rim-Edge model is not responsible for selectivity changes observed here. The absence of any stacking variations between CoMo-C_5 and CoMo-C_6 while strong selectivity changes are observed definitely rules out a selectivity/stacking causality.

The HYD/DDS ratio is not the most appropriate way to evaluate hydrogenolysis *versus* hydrogenating functions since the HYD term corresponds to the HDS product, phenylcyclohexane, which is in fact a secondary product along the HYD pathway formed by C–S bond breaking of an intermediate primary product, THDBT, resulting from the hydrogenation of DBT. Therefore, to use the HYD/DDS ratio will level off differences between hydrogenolysis and hydrogenation functions. These two functions could be better analyzed through the THDBT/BP ratio at similar conversions. This ratio was reported in table 2 for all the catalysts studied here. Up to the CoMo-C_5 catalyst, no real variation of the THDBT/BP ratio could be detected, confirming the absence of any change in selectivity for these catalysts. Interestingly, on moving from CoMo-C_5 to CoMo-C_6, a five-fold decrease of the THDBT/BP ratio is detected, demonstrating a more favored hydrogenolysis function for CoMo-C_6. The HYD/DDS ratio did not allow us to discern this effect since the more favored C–S bond breaking for CoMo-C_6 will increase the rate of formation of PCH at the expense of THDBT, leveling off the variations. This result should be related to a previous study on non-promoted Mo systems prepared under the same conditions [28]. Indeed, the results obtained in the present study agree very well with the previous results concerning the effect of the alkyl length on the selectivity change of Mo systems. Similarly to the present results, a strong change in selectivity was observed on moving from pentyl to hexyl groups with a marked increase in the hydrogenolysis function for Mo catalysts formed from tetrahexylammonium thiomolybdate. This modification was attributed to confinement effects inside the mesopores blocking the sterically demanding adsorption leading to the hydrogenation of the aromatic ring. Indeed, the prerequisite for hydrogenation is a π-complexation through the aromatic ring. This flatwise adsorption covers a large part of the catalyst surface and only rim sites present the suitable geometry for adsorbing reactants. This situation differs strongly from the C–S bond breaking mechanism, which needs only in a more easy way a σ bond between the metal center and the sulfur atom. Hydrogenation of DBT is then a sterically demanding reaction. The steric requirement is not achieved in the mesoporous cavities leading to a confinement effect restricting adsorption on rim sites and changing selectivity. In a parallel situation with Mo systems, using pentyl groups in the precursor leads after *in situ* activation to mesoporosity with an average pore diameter of 30–35 Å without confinement effects, whereas using hexyl groups in the precursor leads to a mesoporous organization shifting to wider pore diameters ($\geq$40 Å) and to confinement effects. This suggests that for pore diameters smaller than 40 Å, particles are not located inside the mesopores.

Finally, the particular "Swiss-cheese"-like morphology observed previously in MoS_2 was also found in the CoMo catalysts, particularly for long alkyl chain precursors as a result of similar decomposition patterns given by both type of precursors. Such morphology is produced by the internal pressure generated by the vaporization of the organic alkyl groups during the decomposition steps of the precursor under high pressure of hydrogen and high temperature of the reaction media. Parallelism may be emphasized between the single-step mode of decomposition of long alkyl chain precursors, the appearance for some of these catalysts of a "Swiss-cheese"-like morphology and the creation of a mesoporous organization. Cavities are produced by the accumulation of gases during the decomposition while channels are created during the escape of gases giving rise to type IV isotherms with well-formed hysteresis loops.

Such a porous network in amorphous materials may be considered equivalent to the porous structure of molecular sieves, which very likely induces confinement effects. Owing to such properties, the high surface area CoMo materials reported in this work are also called "amorphous mesoporous sulfides".

5. Conclusions

CoMo sulfide catalysts (CoMo-R with R = H, C_1, C_4, C_5 and C_6) were prepared by *in situ* decomposition of different tetraalkylammonium thiobimetalate precursors. The solids obtained using this procedure present interesting morphological properties with high surface area and characteristic type IV isotherms with a wide mesoporous distribution and a very dispersed active phase. A synergetic effect of the cobalt promoter is observed when decomposing these bimetallic precursors with a strong enhancement of the direct desulfurization pathway compared with non-promoted Mo systems. The use of carbon-containing precursors leads to a strong increase in the HDS activity with a very favored hydrogenolysis function when using longer alkyl chains in the precursor.

Acknowledgments

The authors appreciate the valuable technical assistance of H. Esparza and A. Reyes. This work was financially supported by Conacyt project J31397-U; FIES-98-27-III.

References

[1] O. Weisser and S. Landa, *Sulfide Catalysts: Their Properties and Application* (Pergamon Press, Oxford, 1973).

[2] H. Topsøe, B.S. Clausen and F.E. Massoth, in: *Catalysis*, *Science and Technology*, vol. 11, eds. J.R. Anderson and M Boudart (Springer, Berlin, 1996).

[3] J.H. Voorhoeve and J.C.M. Stuiver, J. Catal. 23 (1971) 243.

[4] A.L. Farragher and P. Cossee, in: *Proceedings of 5th International Congress on Catalysis*, ed. J.W. Hightower (North-Holland, Amsterdam, 1973), p. 1301.

[5] E. Furimsky, Catal. Rev. Sci. Eng. 22 (1980) 371.

[6] R. Candia, B.S. Clausen and H. Topsøe, J. Catal. 77 (1982) 564.

[7] S. Harris and R.R. Chianelli, J. Catal. 98 (1986) 17.

[8] R.R. Chianelli, G. Berhault, P. Raybaud, S. Kasztelan, J. Hafner and H. Toulhoat, Appl. Catal. A: Gen. 227 (2002) 83.

[9] G. Hagenbach, P. Courty and B. Delmon, J. Catal. 31 (1973) 264.

[10] R. Frety, M. Breysse, M. Lacroix and M. Vrinat, Bull. Soc. Chim. Belg. 93 (1984) 663.

[11] K. Ramanathan and S. Weller, J. Catal. 95 (1985) 249.

[12] M. Zdrazil, Catal. Today 3 (1988) 269.

[13] K. Wilkinson, M.D. Merchán and P.T. Vasudevan, J. Catal. 171 (1997) 325.

[14] E. Frommell, J. Diehl, J. Tamilia and S. Pollack, in: *Proceedings of 12th North American Catalysis Society Meeting*, ed. B.H. Davis, Lexington, KY, 1991, PD-38.

[15] Y. Yoneyama and C. Song, Catal. Today 50 (1999) 19.

[16] S. Fuentes, G. Diaz, F. Pedraza, H. Rojas and N. Rosas, J. Catal. 113 (1988) 535.

[17] K. Inamura and R. Prins, J. Catal. 147 (1994) 515.

[18] A.W. Neummann and A.S. Behan, US Patent 4 243 554 (1981).

[19] R.R. Chianelli and T.A. Pecoraro, US Patent 4 508 847 (1985).

[20] A.J. Jacobson, R.R. Chianelli and T.A. Pecoraro, US Patent 4 650 563 (1987).

[21] T.A. Pecoraro and R.R. Chianelli, US Patent 4 528 089 (1985).

[22] G. Alonso, M. Del Valle, J. Cruz, A. Licea-Claverie, V. Petranovskii and S. Fuentes, Catal. Lett. 52 (1998) 55.

[23] G. Alonso, V. Petranovskii, M. Del Valle, J. Cruz-Reyes, A. Licea-Claverie and S. Fuentes, Appl. Catal. A: Gen. 197 (2000) 87.

[24] G. Berhault, A. Mehta, A.C. Pavel, J. Yang, L. Rendon, M.J. Yácaman, L. Cota, A. Duarte and R.R. Chianelli, J. Catal. 198 (2001) 9.

[25] G. Berhault, L. Cota, A. Duarte, A. Mehta and R.R. Chianelli, Catal. Lett. 78 (2002) 81.

[26] S. Ramanathan and S.T. Oyama, J. Phys. Chem. 99 (1995) 16365.

[27] D.J. Sajkowski and S.T. Oyama, Appl. Catal. A: Gen. 134 (1996) 339.

[28] G. Alonso, G. Berhault, A. Aguilar, V. Collins, C. Ornelas, S. Fuentes and R.R. Chianelli, J. Catal. 208 (2002) 359.

[29] G. Alonso, G. Aguirre, I.A. Rivero and S. Fuentes, Inorg. Chim. Acta 274 (1998) 108.

[30] G. Alonso, G. Berhault and R.R. Chianelli, Inorg. Chim. Acta 316 (2001) 105.

[31] G. Alonso, J. Yang, M.H. Siadati and R.R. Chianelli, Inorg. Chim. Acta 325 (2001) 193.

[32] W.-H. Pan, D.C. Johnston, S.T. McKenna, R.R. Chianelli, T.R. Halbert, L.L. Hutching and E.I. Stiefel, Inorg. Chim. Acta 97 (1985) L17.

[33] K.S. Liang, R.R. Chianelli, F.Z. Chien and S.C. Moss, J. Non-Cryst. Solids 79 (1986) 251.

[34] D.D. Whitehurst, T. Isoda and I. Mochida, Adv. Catal. 42 (1998) 345.

[35] R.R. Chianelli and G. Berhault, Catal. Today 53 (1999) 357.

[36] V. Schwartz, V. Teixeira da Silva and S.T. Oyama, J. Mol. Chem. A: Chem. 163 (2000) 251.

[37] B. Dhandapani, T. St Clair and S.T. Oyama, Appl. Catal. A: Gen. 168 (1998) 219.

[38] A.S. Mamède, J.M. Giraudon, A. Löfberg, L. Leclercq and G. Leclercq, Appl. Catal. A: Gen. 227 (2002) 73.

[39] F. Bataille, J.-L. Lemberton, P. Michaud, G. Pérot, M. Vrinat, M. Lemaire, E. Schulz, M. Breysse and S. Kasztelan, J. Catal. 191 (2000) 409.

[40] M. Breysse, G. Berhault, S. Kasztelan, M. Lacroix, F. Maugé and G. Pérot, Catal. Today 66 (2001) 15.

[41] G. Berhault, M. Lacroix, M. Breysse, F. Maugé, J.-C. Lavalley, H. Nie and L. Qu, J. Catal. 178 (1998) 555.

[42] M. Daage and R.R. Chianelli, J. Catal. 149 (1994) 414.